Supporting Information

Computational design of nanostructured soft interfaces: focus on shape changes and spreading of cubic nanogels

Chandan Kumar Choudhury, Vaibhav Palkar, Olga Kuksenok[*]

Department of Materials Science and Engineering, Clemson University,
Clemson, South Carolina 29634, USA

*E-mail: okuksen@clemson.edu

*Phone: 1-864-656-5956

$I \times J \times K$	# of cross-link beads	# of beads between cross-links, N_x	Total # of acrylamide beads	Shape
$2 \times 2 \times 2$	45	48, 30,25,20,15	6144, 3840, 3200, 2560, 1920	Cubical
$3 \times 3 \times 3$	170	14, 30,25,20,15	6048, 12960, 10800, 8640, 6480	Cubical
$4 \times 4 \times 4$	427	6, 30,25,20,15	6144, 30720, 25600, 20480, 15360	Cubical
$3 \times 3 \times 3$	106	30	6708	Spherical
$5 \times 5 \times 5$	492	6	6224	Spherical

Table S1. Details of hydrogels geometries

a_{ij}	Polymer (P)	Oil (O)	Water (W)	Solvent (S)
Polymer (P)	78			
Oil (O)	85	78		
Water (W)	85	100	78	
Solvent (S)	80,90,95	100		78

Table S2. Repulsion parameters used in simulations; parameters assigned to cross-linker beads are the same as those for polymers

	N_x	Total number of gel beads	Box dimensions	Total number of beads in box
$2 \times 2 \times 2$	*48*	*6235*	*100 x 95 x 100*	*2,850,000*
	30	3931	85 x 95 x 85	2,059,125
	25	3291	75 x 70 x 75	1,181,250
	20	2651	60 x 50 x 60	540,000
	15	2011	55 x 50 x 55	453,750
$3 \times 3 \times 3$	30	13226	120 x 120 x 120	5,184,000
	25	11076	100 x 85 x 100	2,550,000
	20	8916	95 x 85 x 95	2,301,375
	15	6756	75 x 60 x 75	1,012,500
	14	*6324*	*75 x 60 x 75*	*1,012,500*
	30	**6844**	**95 x 95 x 95**	**2,572,125**
$4 \times 4 \times 4$	30	31337	150 x 150 x 150	10,125,000
	25	26217	120 x 150 x 120	6,480,000
	20	21097	110 x 140 x 110	5,082,000
	15	15977	80 x 90 x 80	1,728,000
	6	*6761*	*50 x 60 x 50*	*450,000*
$5 \times 5 \times 5$	**6**	**6760**	**50 x 60 x 50**	**450,000**

Table S3. Number of beads and box dimensions for polymer, oil, and solvent beads. The shaded parameters are also used for equilibrium simulations of polymer gel in water. The bold entries are for spherical gels. Italic entries are also used for simulation of multiple gels. Box size for multiple gels simulation was modified to 60 x 100 x 60 for $2 \times 2 \times 2$ gels and 50 x 80 x 50 for $3 \times 3 \times 3$ and $4 \times 4 \times 4$ gels.
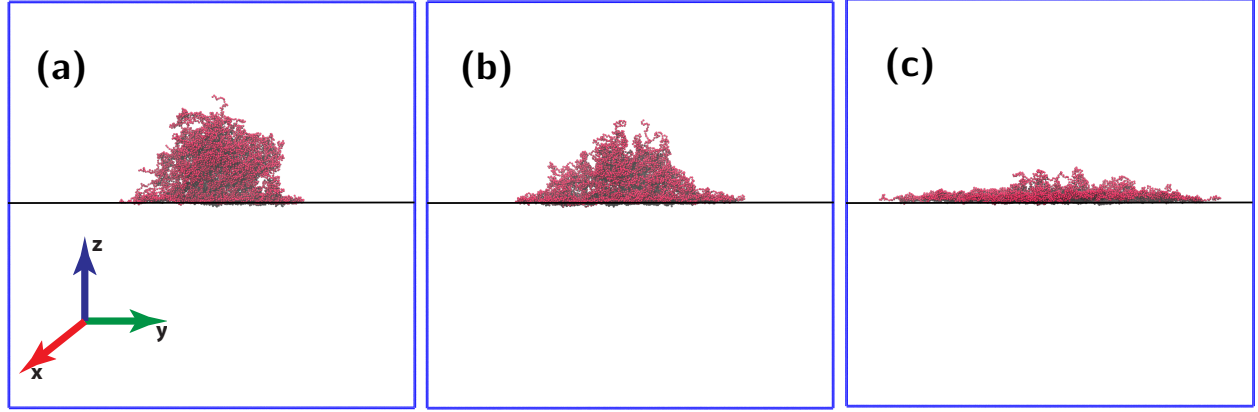
Figure S1. (a-c) A side view of the snapshots for $3 \times 3 \times 3$ $N_x = 30$ gel as it adsorbs onto the oil-water interface at: (a) 1.17×10^4, (b) 1.43×10^4, and (c) $6 \times 10^4 \tau$. Here oil and water beads are hidden to highlight the spreading at the interface. Black line represents the interface.
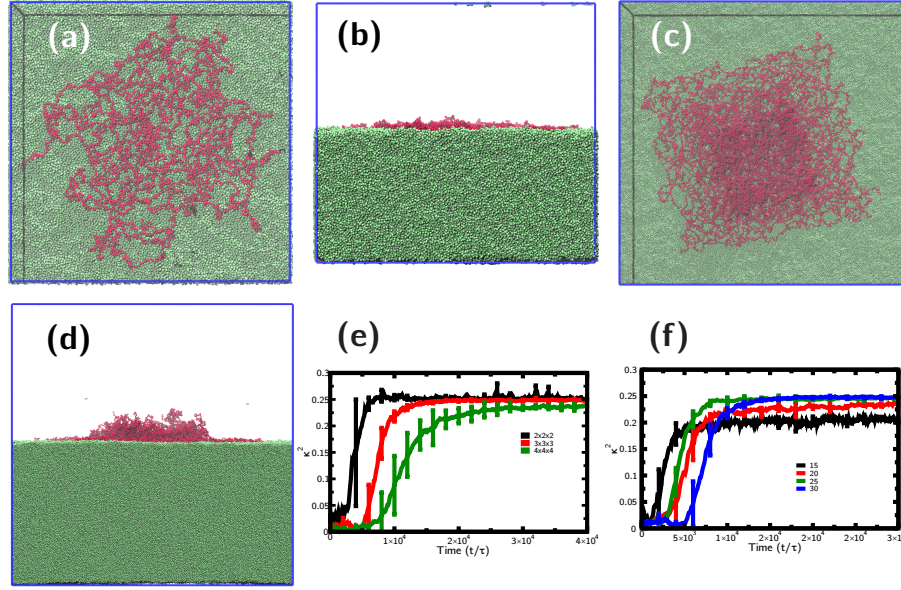
Figure S2. Equilibrium morphology snapshots for $N_x = 30$, $2 \times 2 \times 2$ gels in (a, b) and $N_x = 30$, $4 \times 4 \times 4$ gels in (c,d). (a, c), and (b,d) are top ($\boldsymbol{xy}$-plane) and side views ($\boldsymbol{yz}$-plane) respectively. (e,f) Time evolution of shape anisotropy κ^2 for (e) $2 \times 2 \times 2$, $3 \times 3 \times 3$ and $4 \times 4 \times 4$ $N_x = 30$; (f) $3 \times 3 \times 3$, $N_x = 15, 20, 25, 30$. Time $t = 0$ in (e,f) corresponds to the time instant gel contacts the oil-water interface.
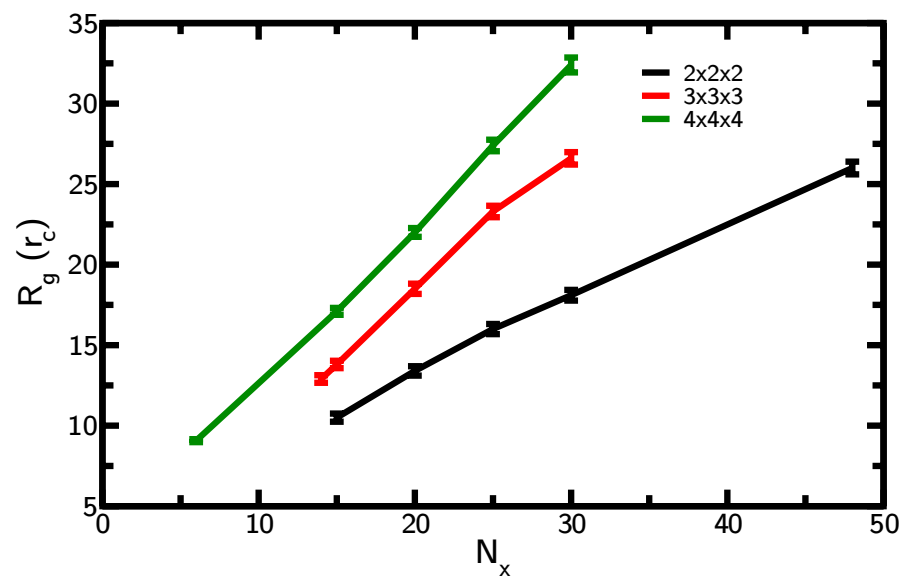
Figure S3. Equilibrium radius of gyration, R_g, for $2 \times 2 \times 2$, $3 \times 3 \times 3$ and $4 \times 4 \times 4$ gels adsorbed at the oil-water interface.
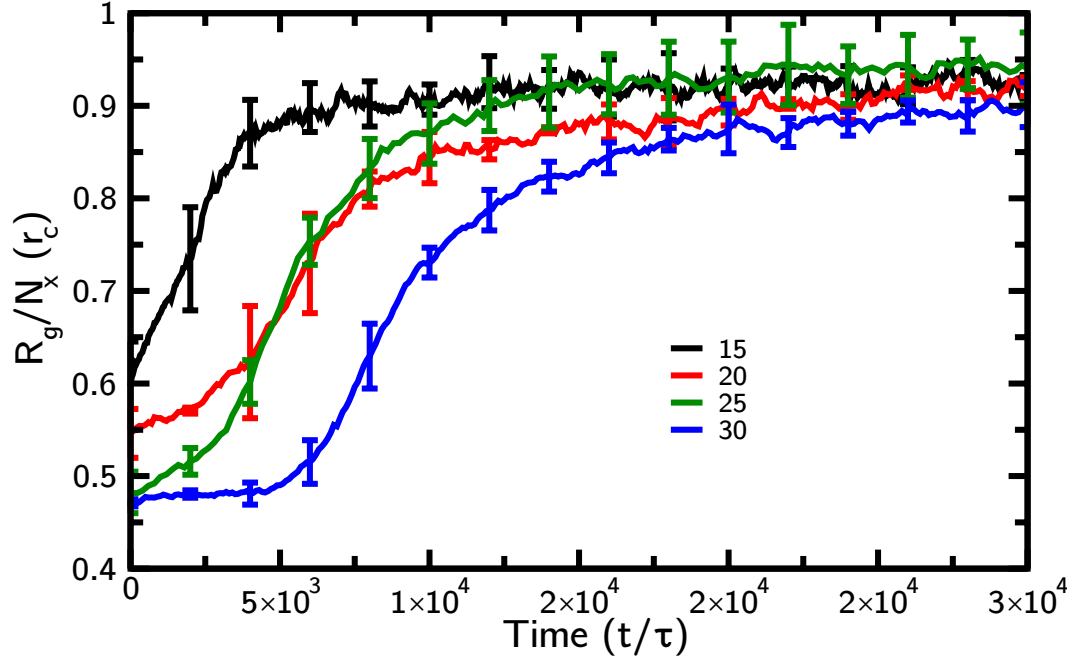
Figure S4. Time evolution of normalized radius of gyration R_g/N_x for $3 \times 3 \times 3$ gels during adsorption onto the oil-water interface for $N_x = 15, 20, 25, 30$. Time $t = 0$ corresponds to the time instant gel contacts the oil-water interface.
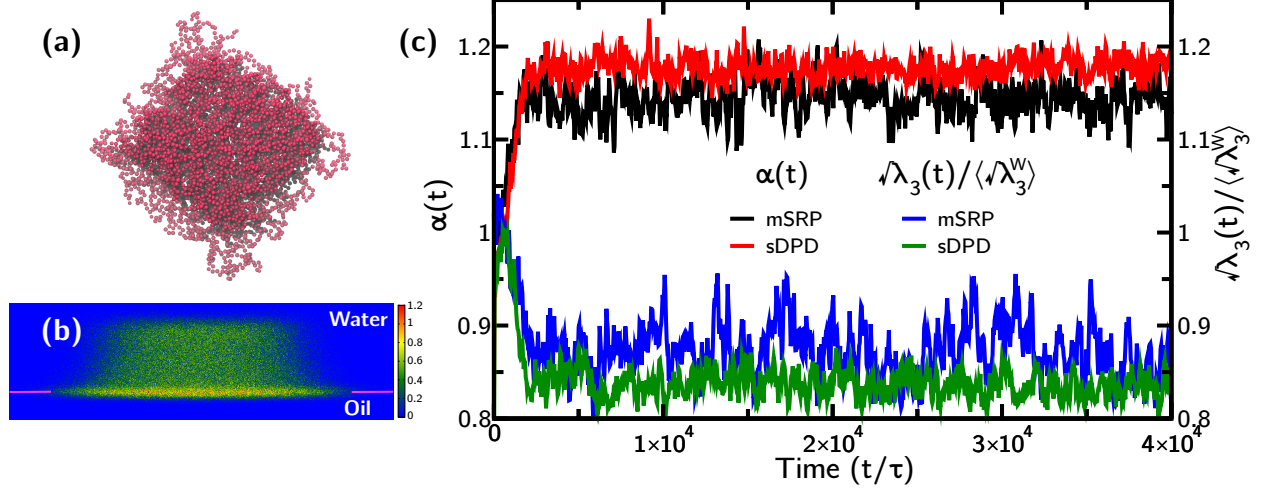
Figure S5. (a,b) An equilibrium gel morphology (top view, an interface is not shown) and polymer density for $4 \times 4 \times 4$, $N_x = 6$ (side view, close-up around the gel only) (c) Time evolution of an extent of spreading, $\alpha(t)$, (red and black lines, left axis) and an effective change in thickness, $\sqrt{\lambda_3}(t)/< \sqrt{\lambda_3^W} >$, (blue and green lines, right axis). Figures a,b, and black and blue lines in (c) are obtained using the modified segmental repulsion potential (mSRP) DPD approach. Red and green lines in (c) are from the regular standard DPD simulations (sDPD, as mentioned in the model section). We implemented mSRP[1] potentials on polymer beads, to minimize the effect of bond crossing. This potential is defined as

$$F_{ij}^{mSRP} = \begin{cases} a_{ij}^E \left(1 - \dfrac{d_{ij}}{d_c}\right) \boldsymbol{d}_{ij} & (d_{ij} < d_c) \\ 0 & (d_{ij} \geq d_c) \end{cases}$$

where F_{ij}^{mSRP} is a force acting between bonds i and j, separated by distance d_{ij}, d_c is the cut-off distance and a_{ij}^E is the force constant. We use $d_c = 0.8\, r_c$, and $a_{ij}^E = 80\, k_B T/r_c$ (same value as implemented in Ref. 1). An extent of spreading, $< \alpha >$, for gels with mSRP and sDPD, in equilibrium reaches 1.14 and 1.16 respectively, while the average value of the effective thickness (normalized by the corresponding linear dimension in water) is 0.87 and 0.84 for mSRP and sDPD, respectively. The (a) and (b) images here are with the implementation of the mSRP framework (to be compared with the corresponding snapshots in Figure 4 e,f of the main text corresponding to the sDPD approach). These results show that these characteristics as well as an overall shape of the gel at the interface remain essentially unaffected.
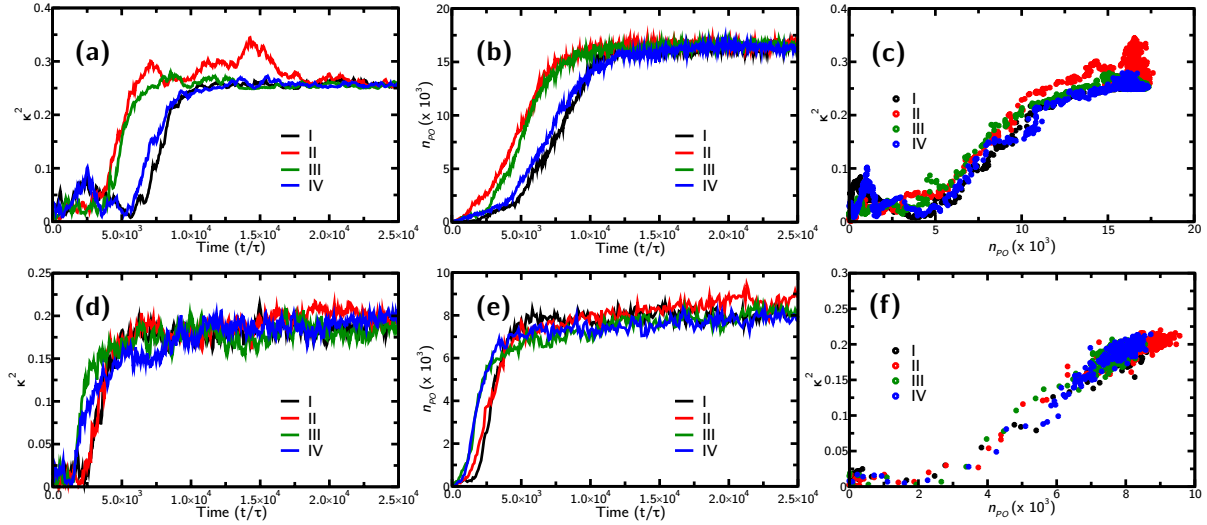
Figure S6. (a-c) Time evolution of κ^2 in (a), a number of contacts in (b) and a parametric plot $\kappa^2(n_{po})$ using the data in (a) and (b) in (c) for gel $2 \times 2 \times 2$, $N_x = 48$. **(d-f)** Time evolution of κ^2 in (d), a number of contacts in (e) and a parametric plot $\kappa^2(n_{po})$ using the data in (d) and (e) in (f) for gel $3 \times 3 \times 3$, $N_x = 14$. Different colors represent data from independent simulation runs with varying initial random velocities. Data in (c) and (f) are averaged over four runs and are used to plot black and red curves in Figure 5c, where black curve is superimposed onto the red and green curves. Note that loosely cross-linked gels ($N_x = 48$) allow for larger fluctuations in the number of contacts; in some of the cases with $N_x = 48$ only we observed the number of contacts increased to a small value and then decreased back to zero, corresponding to only a short contact with a fraction of polymer chain. Hence, we have counted time $t = 0$ in the above plots from the time gels contact the interface and remain in contact with the interface.
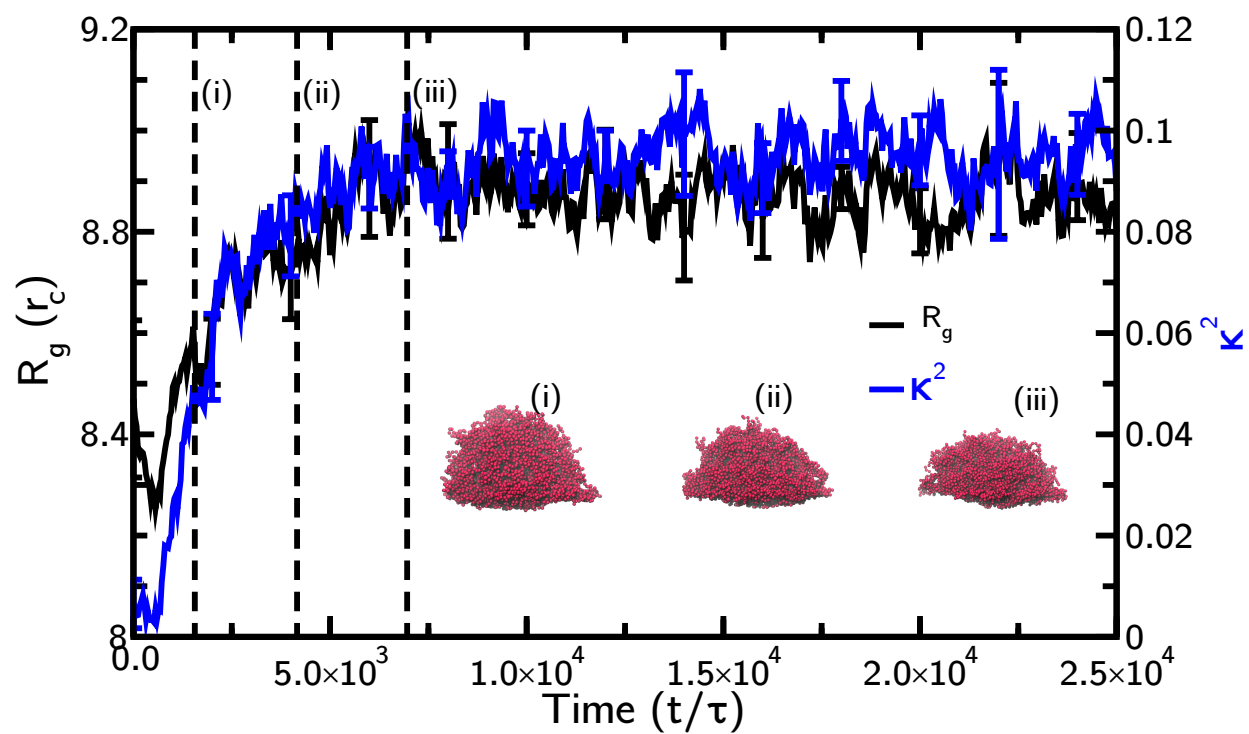
Figure S7. Time evolution of R_g (black line) and κ^2 (blue line) for a $5 \times 5 \times 5$ $N_x = 6$ spherical gel during adsorption onto the oil-water interface. Inset shows intermediate gel morphologies at (i) 1.56, (ii) 4.16 and (iii) 6.76×10^3 τ.
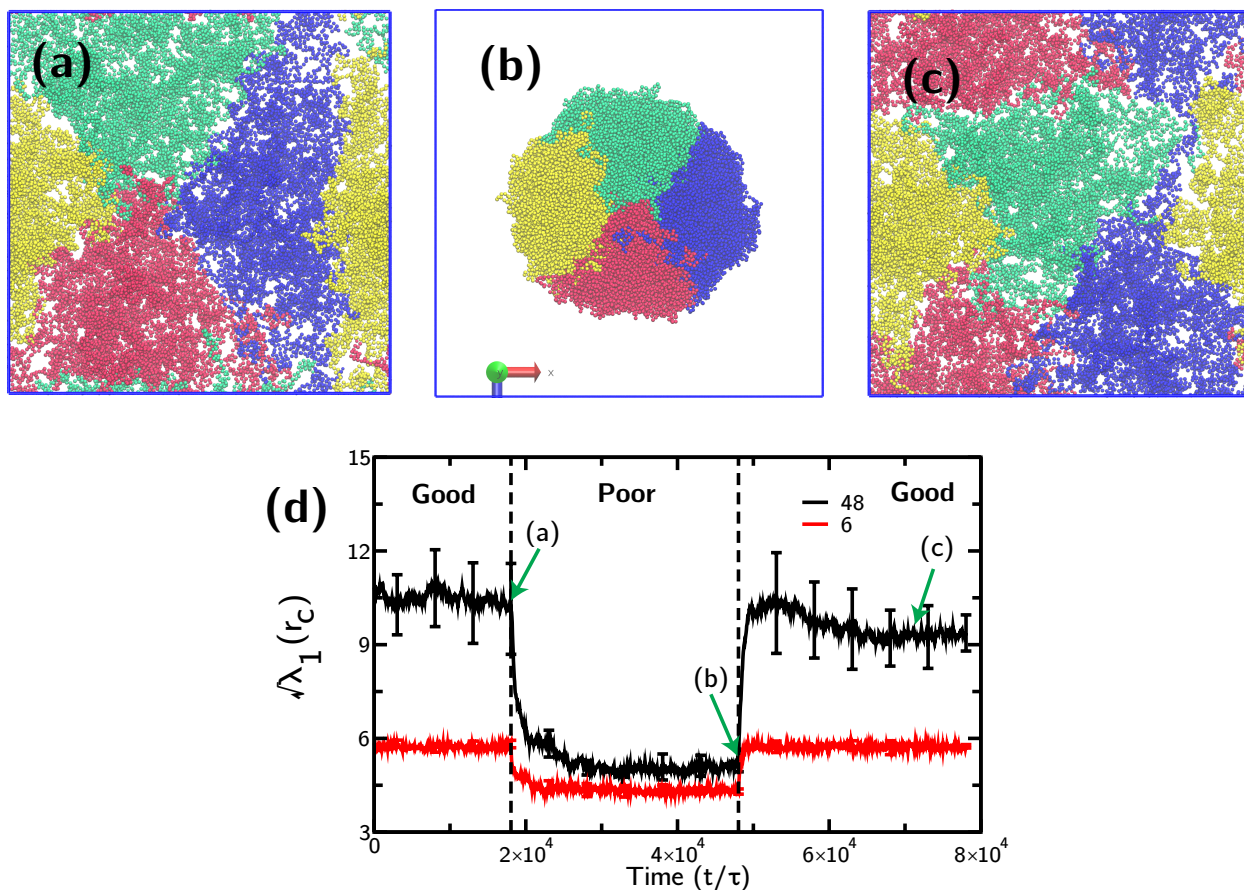
Figure S8. (a-c) Shape changes and aggregation of gels at interface upon changing the solvent quality from good ($a_{PS} = 80$) to poor ($a_{PS} = 95$) for $2 \times 2 \times 2, N_x = 48$. For clarity, the interface is not shown here. The morphology snapshots correspond to the time instances $t = 1.804, 4.804, 6.804 \times 10^4 \tau$ (from left to right). Four gels are colored differently to show their respective conformations. (d) Evolution of $\sqrt{\lambda_1}$ with change in solvent quality. Data are averaged over four gels. The gel conformation in a good solvent is the same as shown in Figure 8a.

References

1.   Sirk, T. W.; Slizoberg, Y. R.; Brennan, J. K.; Lisal, M.; Andzelm, J. W., An enhanced entangled polymer model for dissipative particle dynamics. *J. Chem. Phys.* **2012,** *136* (13), 134903.